This article has been accepted for publication in IEEE Internet of Things Journal. This is the author's version which has not been fully edited and content may change prior to final publication. Citation information: DOI 10.1109/JIOT.2024.3491182

Tackling Hidden Node Problem Utilizing Traffic Periodicity and Downlink Carrier Sense in LPWAN

Aoto Kaburaki, *Graduate Student Member, IEEE,* Koichi Adachi, *Senior Member, IEEE,* and Osamu Takyu, *Member, IEEE,*

***Abstract*—Low-power wide-area networks (LPWANs), which achieve low-power consumption, enabling long-term battery operation and long-range communication capabilities, have emerged as a new standard for realizing massive wireless sensor networks (WSN). LPWANs are becoming increasingly popular due to low introduction costs, which stem from features such as using unlicensed bands and low-cost nodes. LPWANs are particularly useful for Internet-of-Things (IoT) applications that periodically collect information about specific observation targets. However, LPWAN generally adopts a simple medium access control (MAC), which significantly degrades communication quality due to packet collisions when the traffic load increases. Thus, MAC design is critical for realizing large-scale LPWANs. Carrier sense multiple access (CSMA) can autonomously avoid packet collisions. However, its performance is drastically deteriorated due to the hidden node problem in large-scale LPWANs. This paper proposes an autonomous distributed MAC strategy that can suppress the hidden node problem by utilizing traffic periodicity. The proposed method is designed carefully considering LPWAN-specific constraints, such as duty cycle limitations in unlicensed bands, low clock accuracy of nodes, and limited downlink communication opportunities. From numerical results, the proposed method improves the packet delivery rate (PDR) performance by up to approximately by 29%, 9% and 8% compared to ALOHA, CSMA-x, and the state-of-the-art LoRa MAC, respectively.**

***Index Terms*—Internet of Things (IoT), LoRaWAN, low-power wide area networks (LPWAN), resource allocation.**

I. Introduction

With the development of wireless communication technology, a new framework known as the Internet-of-Things (IoT) is rapidly spreading. IoT is being adopted in various applications and is expected to be a transformative technology, enabling ubiquitous connectivity and data exchange between a vast array of devices and systems. Examples of IoT applications include smart home automation, smart cities, industrial and environment monitoring systems, and safety/security solutions, among others [1], [2]. In these applications, wireless sensor networks (WSNs) are constructed by sensors with wireless communication functions. On top of broadly known standards, such as Bluetooth; Wi-Fi; and ZigBee, that can construct WSNs, a new paradigm; low power wide area networks (LPWAN), has emerged in recent years [3], [4]. LPWAN has gained significant traction because of its capability to offer a promising solution for applications that require extended coverage, low power consumption, and cost-effective scalability [2], [5]–[9].

LPWAN is designed to facilitate the transmission of small data packets over long distances, typically up to several kilometers, while operating on batteries for an extended time. In many applications adopting LPWAN, such as smart city infrastructure monitoring and smart agriculture systems, strategically deploying wireless sensor nodes across a designated area is a common practice. The primary purpose of these sensor nodes is to sense and monitor the surrounding environmental conditions. Subsequently, the nodes transmit their recorded observation data periodically to an information aggregation station, typically a gateway (GW). Consequently, the network traffic patterns tend to be dominated by periodic uplink (UL) transmissions in LPWAN [10]–[12]. Especially in LPWAN, accommodating potentially thousands of nodes and efficiently collecting the UL data flows from them is crucial for reliable operation and scalability. As a result, this characteristic of UL-dominated and periodic data flows is a crucial factor that demands careful consideration during the design of medium access control (MAC) protocols for LPWAN.

Efficient MAC protocols have been actively studied for LPWAN, especially in LoRaWAN, which is an open standard [12]–[23]. As centralized MAC protocols, scheduling methods and frequency channel allocation have been studied [24], [25]. As distributed MAC protocols, listen-before-talk (LBT) methods like carrier sense multiple access/collision avoidance (CSMA/CA) and resource selection utilizing machine learning (ML) have been investigated. However, ALOHA protocol is still widely used as a compromise solution, albeit reluctantly, due to the overhead associated with control signal exchange in centralized control methods. Also, when the communication area is large, distributed MAC protocols suffers from the hidden node problem. In addition, continuous packet collisions may manifest for periodic UL traffic, contingent upon the specific combination of transmission cycles across the various nodes. If the transmission cycles of multiple nodes align, their respective packets will persistently collide, leading to frequent data loss. Continuous packet collisions can significantly impair the fresh update of information at the GW, leading to a degradation in delay performance such as age-of-information (AoI) [25]–[28]. Consequently, LPWAN requires a novel MAC protocol that factors in the periodic traffic, in other words, a resource allocation strategy.

Manuscript received April 19, 2005; revised August 26, 2015. This research is supported by JSPS KAKENHI Grant Numbers 23KJ0965. In addition, this research is supported in part by the MIC/SCOPE JP235004002.

A. Kaburaki and K. Adachi are with Advanced Wireless and Communication Research Center (AWCC), The University of Electro-Communications, 1-5-1 Chofugaoka, Chofu, Tokyo 182-8585, Japan (e-mail: kaburaki@awcc.uec.ac.jp).

O. Takyu is with the Department of Electrical and Computer Engineering, Faculty of Engineering, Shinshu University, 4-17-1, Wakasato, Nagano 380-8553, Japan.

When designing wireless resource allocation strategies for LPWAN, there are three crucial factors that demand careful consideration. The first factor is the duty cycle (DC) constraint. Notably, unlicensed LPWAN offers highly scalable and cost-effective solutions by leveraging unlicensed frequency bands and employing inexpensive nodes. Among the unlicensed LPWAN technologies, LoRaWAN has garnered widespread adoption due to its flexibility and scalability [5]. However, a wireless resource usage limitation exists, known as the DC constraint, in terms of frequency band sharing with other systems. The DC constraint specifies the maximum permissible ratio of transmission time to a predetermined period, during which a transmitter can use a specific frequency channel. The second is downlink (DL) receive period limitation. General LPWAN standards either do not support DL communication strictly limit the timing for DL communication from the standpoint of node power saving. For example, LoRaWAN Class A nodes, which are designed for battery operation, must open a DL receive window for a certain period after UL transmission only. The DL receive window is not open during the rest of the time, and DL messages cannot be received. The third factor is clock drift. Generally, LPWAN nodes employ inexpensive circuit components, including low-precision crystal oscillators, for their internal clocks [8]. These oscillators are susceptible to accuracy fluctuations caused by environmental factors like temperature variations and the effects of aging. Consequently, the clock values may unintentionally deviate from their intended values [29]. Over time, this leads to the accumulation of a time difference between the clocks of the transmitting and receiving nodes that are called clock drift [18], [30]–[32].

A. Related Studies

In LPWANs, the design guidelines for resource allocation strategies vary greatly depending on whether time synchronization is assumed or not. A packet collision avoidance method that requires time synchronization is proposed in [24], [33], [34]. These methods utilize the time domain wireless resources effectively by transmitting synchronization signals such as acknowledgement (ACK) and broadcast beacons to perform time synchronization. Time synchronization realizes a higher PDR compared to the conventional ALOHA protocol. As discussed in [35], the number of devices that can be synchronized is limited by DC constraints and the amount of clock drift. For this reason, the number of nodes that can be supported by the methods [24], [33], [34] are likely to be significantly limited. In [19], the authors proposed a centralized control resource allocation strategy that does not require strict synchronization. In this method, the GW controls the transmission timing and the frequency channel used by each node, taking into account the transmission cycle of each node, the effect of clock drift, and the DC constraints on DL control signal transmission. Since it is still necessary to transmit control signals to the nodes for resource allocation, the effectiveness of the proposed method decreases in environments with a large number of nodes.

On the other hand, there are many resource allocation strategies that do not require time synchronization [20], [36]–[41]. These methods are basically based on LBT. In [20], [36]–[38], distributed MAC protocols inspired by CSMA/CA used in conventional IEEE 802.11 networks are proposed. CSMA-x, which is a simplified version of the CSMA/CA protocol (i.e., non-persistent carrier sense multiple access (NP-CSMA)) adapted for LoRaWAN, is proposed in [36]. In the CSMA-x protocol, a node assesses the status of the frequency channel for a duration of x milliseconds before transmitting a packet. In [37], [38], a LoRa MAC (LMAC) protocol is proposed. LMAC is designed to be more suitable for LoRaWAN than CSMA-x and was adopted as an industry standard by the LoRa Alliance in 2023. In January 2024, LMAC was also published as the default for CSMA in the official LoRaWAN library [42]. In LMAC, each node calculates the frequency channel occupancy based on the status information of the frequency channels observed by the CS. Selecting the frequency channel based on their occupancy can distribute UL traffic to each channel, leading to the suppression of packet collisions. However, these LBT-based methods still suffer from the hidden node problem in the case of wide communication areas [20].

The request-to-send/clear-to-send (RTS/CTS) is widely known as a solution to the hidden node problem [8], [39]–[41], [43]. In general, RTS/CTS requires a node to always keep its receive window open to receive RTS/CTS packets, which is likely to be inapplicable to battery-powered nodes [43]. Thus, an RTS-LoRa and LoRa mode adaptive protocol (LoRa-MAP) is proposed in [39], [40]. These methods do not require CTS packets, thus reducing overhead compared to [43]. Also, in [41], a probabilistic RTS method is proposed to reduce the collision rate of RTS packets. In this way, many studies have used RTS to avoid hidden node problems. However, there are fundamental issues that should not be ignored, such as the degradation of frequency efficiency caused by RTS packet transmission, collisions of RTS packets, and the increase in power consumption of nodes caused by listening to RTS packets.

B. Objective and Main Contributions of This Study

In [44], we proposed a distributed resource allocation method that tackles the hidden node problem. A carrier sense (CS) aimed at detecting DL is considered, which is also the focus of this paper, to design resource allocation in the time and frequency domains. Computer simulation results demonstrate that this method can suppress packet collisions due to the hidden node problem. However, since [44] considers a simplified signal detection model, it may not be robust to the effects of noise and interference. Furthermore, resource allocation in the time domain may not function properly when clock drift occurs.

Therefore, from a more practical point of view, LPWAN requires resource allocation strategies that consider a cross-layer approach from the application to the hardware, such as periodic traffic caused by the applied application; DC constraints caused by the frequency band used; low power consumption that allows battery operation; and clock drift caused by low-cost circuits. Furthermore, many LPWAN systems require nodes to be battery-powered. Consequently, the number of active nodes may unintentionally change due to factors such as battery depletion. The change of the active nodes leads to dynamic changes in network topology and traffic, making robustness to such changes an essential aspect of MAC protocols in LPWAN.

Thus, the objective of this paper is to design a packet collision avoidance resource allocation strategy that accounts for these constraints of LPWAN. We focus on two points. First, controlling the nodes prone to the hidden node problem in LBT-based LPWAN is more efficient than controlling all nodes in the network. Second, since the DL receive windows of LPWAN nodes typically open at predetermined times, the DL receive windows of node pairs causing packet collisions are likely to overlap. Thus, a single DL packet may transmit information to multiple nodes without synchronization if properly designed. With this background, this paper proposes a distributed sequential resource allocation strategy to reduce packet collisions caused by the hidden node problem. Computer simulation results show that the proposed method can improve the packet delivery rate (PDR) by 29%, 9% and 8% compared with the pure-ALOHA protocol, CSMA-x protocol [36], and LMAC protocol [38] respectively.

The main advantages of the proposed method are as follows.

(i) The proposed method is able to improve the PDR while fully adhering to many constraints in LPWAN.

(ii) By taking advantage of traffic periodicity and CS, nodes can implicitly sense the presence of hidden nodes. In particular, this method does not require complex processing at the node.

(iii) The proposed method adopts a sequential resource allocation strategy triggered by DL packets without control information, making it robust to changes in network topology.

The remainder of this paper is organized as follows. Section II describes the LoRaWAN-based system model. The proposed method is presented in Section III. Section IV provides computer simulation results. Section V concludes the paper.

II. System Model

This study adopts the widely studied LoRaWAN-based system model, a popular choice among LPWAN technologies. The physical layer of LoRaWAN adopts LoRa modulation, also known as the frequency shift chirp modulation (FSCM). LoRa modulation provides robustness to interference by spreading narrowband signals over the system bandwidth [45].

A. Network Model

Our network model is a star topology consisting of I LoRaWAN nodes (represented by the set $\mathcal{I} = \{1, \cdots, i, \cdots, I\}$) and a single GW, as shown in Figure 1. Each node selects a single orthogonal frequency channel from the set of available channels ($\mathcal{K} = \{1, \cdots, k, \cdots, K\}$) to transmit UL packets and receive DL packets. On the other hand, the GW supports multi-channel operation, i.e., simultaneous DL transmission and simultaneous UL reception can be performed for all frequency channels. All nodes and the GW operate in a half-duplex mode, which means that transmission and reception can not be performed simultaneously.

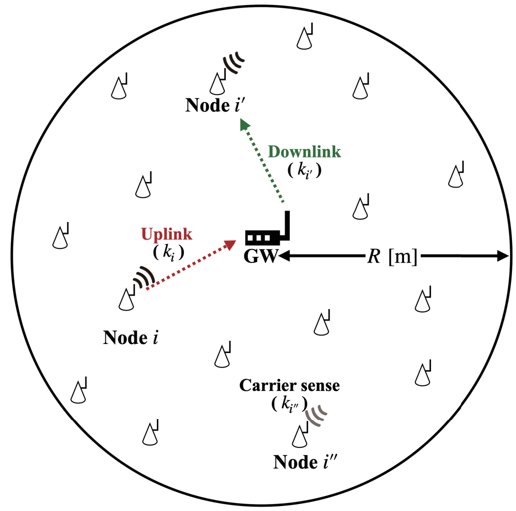

Fig. 1. System model

B. Packet Transmission in LoRaWAN

The LoRaWAN packet consists of a preamble, synchronization word, physical header (PHDR), header cyclic redundancy check (CRC), physical payload, and payload CRC [46]. In particular, the physical payload includes the following of the node: device address (DevAddr), frame counter (FCnt), and application payload. FCnt is a count-up value for each packet transmission for each node, which indicates the number of UL packets transmitted by the node. Each packet contains the CSS symbols generated by LoRa modulation. LoRa modulation adaptively changes the data rate according to the received power level through a crucial parameter called SF. The selection of the SF parameter in LoRa modulation is a crucial decision, as it directly impacts the data rate and the minimum required received power level. As the SF value increases, the data rate decreases, but the minimum required received power level also decreases, presenting a trade-off. SF value is selected from integer values ranging from 7 to 12 (represented by the set $\mathcal{S} = \{7, 8, \cdots, 12\}$), which determines the number of bits transmitted by a single CSS symbol [47]. When a node i selects an SF value $S_i \in \mathcal{S}$, the length of one CSS symbol $T_i^{\mathrm{s}}(S_i)$ [s] is expressed as

$$T_i^{\mathrm{s}}(S_i) = 2^{S_i}/W, \tag{1}$$

where W [Hz] is the frequency bandwidth. The number of CSS symbols in one LoRaWAN packet is expressed as [48]

$$N_i^{\mathrm{s}}(S_i) = O_{\mathrm{sym}} + \left\lceil \frac{B_{\mathrm{data}}/R_{\mathrm{code}}}{S_i} \right\rceil, \tag{2}$$

where $\lceil x \rceil$ is the ceiling function of x, O_{sym} is the number of symbols required for transmission in addition to the physical payload and CRC, B_{data} [bit] is the data size of the physical payload and CRC, and R_{code} is the coding rate. Without loss of generality, this paper assumes that the packet structure of all nodes and the GW are the same. Thus, the time-on-air (ToA) per packet for node i, denoted as T_i^{ToA} [sec], is expressed as

$$T_i^{\mathrm{ToA}} = T_i^{\mathrm{s}}(S_i) \times N_i^{\mathrm{s}}(S_i). \tag{3}$$

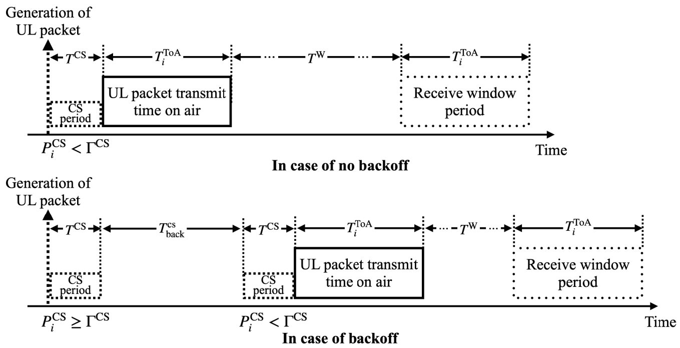

Fig. 2. Behavior of node after packet generation

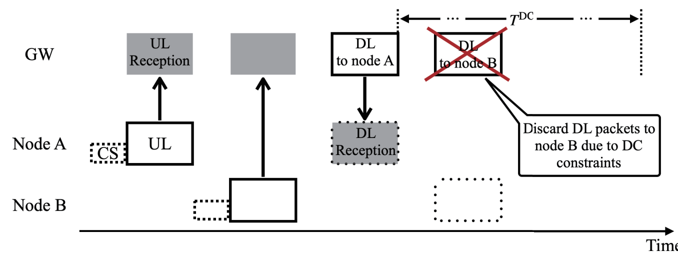

Fig. 3. DC constraints for DL packets in a specific frequency channel

C. Operation at LoRaWAN Node

This subsection describes the operation at the node, i.e., from the UL packet generation to the receive window, as defined without the influence of clock drift. The impact of clock drift and its model will be explained in Section II-F.

1) UL packet generation: This paper focuses on periodic UL traffic, which is common for environmental monitoring, smart farms, etc [10], [11]. Node i is assumed to generate a UL packet at a predetermined cycle of G_i^{p} [min] and transmit the generated packet to the GW. The value $G_i^{\mathrm{p}} \in [1, 2, \cdots, G_{\max}^{\mathrm{p}}]$ is determined before the nodes are placed. Note that the first packet generation time is randomly selected from $[0, \cdots, G_{\max}^{\mathrm{p}}]$.

2) LBT and Backoff: A concise overview of the operation of LBT and backoff are provided, which serves as the foundation for the proposed scheme. This paper focuses on CSMA-x [36] among the various LBT-based schemes [49]. LoRaWAN nodes perform CSMA-x-based transmission timing control. Once node i generates a UL packet, it performs CS for T^{CS} [msec] [ms] before UL packet transmission. If node i observes power value P_i^{CS} greater than or equal to Γ^{CS} [dBm] during CS period T^{CS}, node i judges that the sensed frequency channel is currently being in use. Then, the node initiates a backoff procedure. Backoff waiting time $T_{\mathrm{back}}^{\mathrm{cs}}$ [sec] is expressed as

$$T_{\mathrm{back}}^{\mathrm{cs}} = \mathcal{U}\left(1, 2^{n_{\min}^{\mathrm{CS}} + n_{\mathrm{r}}^{\mathrm{CS}}}\right), \tag{4}$$

where $n_{\min}^{\mathrm{CS}}$ is the minimum backoff exponent, and $n_{\mathrm{r}}^{\mathrm{CS}}$ indicates the backoff count for the m-th packet. Backoff procedure occurs until $n_{\min}^{\mathrm{CS}} + n_{\mathrm{r}}^{\mathrm{CS}} \leq N_{\max}^{\mathrm{CS}}$, where $N_{\max}^{\mathrm{CS}}$ is the maximum backoff exponent. If node i observes power value P_i^{CS} [dBm] less than the CS threshold value Γ^{CS} [dBm], the node immediately transmits the UL packet using frequency channel $k_i \in \mathcal{K}$ and SF $S_i \in \mathcal{S}$ once CS period is over. Here, SF S_i is allocated based on the SNR value at the GW [50]. This paper assumes that all UL packets are transmitted as an unconfirmed message, which does not require an ACK from the GW.

3) Receive Window Opening: A LoRaWAN node opens the receive window at a predetermined T^{w} [sec] after the UL packet transmission [51]. In addition, the receive window shall be open for the time length same as the UL packet ToA T_i^{ToA}. This paper assumes that DL packets are successfully received by node i if the GW transmits them while the node opens the receive window. Figure 2 shows the brief summary of the operation of a node from UL packet generation to the receive window opening.

D. Operation at GW

This subsection provides information on how the GW performs UL reception and DL transmission.

1) Packet Reception Model: Since the available frequency channels are orthogonal, the reception process is defined on an individual frequency channel. Suppose one node is transmitting a UL packet on a particular frequency channel. The reception is successful if the signal-to-noise power ratio (SNR) of the UL packet at the GW is greater than SNR threshold Γ^{SNR}. As a characteristic of LoRa modulation, the SNR threshold required for successful reception is different for different SF values [50]. Now consider the case where multiple nodes transmit UL packets on the same frequency channel with overlapping packet transmission durations. Since the nodes are operating asynchronously, the probability that the GW starts multiple UL packet reception at the same time is extremely small. Packet collisions are modeled based on the situation where the GW is receiving and processing a UL packet. In other words, while receiving and processing one packet, another UL packet arrives and interferes with the reception and processing. In particular, the GW performs demodulation by synchronizing to the preamble of the first arriving packet. In this paper, even in the case of packet collision, the packet is successfully received if the SNR and SIR of the first packet arriving at the GW exceed the respective threshold values Γ^{SNR} and Γ^{SIR} due to the capture effect [52], [53].

2) DL Packet Transmission: The GW can transmit DL packets if it is not processing UL packet reception on all frequency channels. Upon successful packet reception from node i, the GW can transmit a DL packet to node i, using the same SF S_i and frequency channel k_i as node i. Since waiting time T^{w} until the node opens the receive window i is known in advance, the GW easily estimates the window open period at node i. In this paper, the DL packet ToA is assumed to be the same as the corresponding UL packet.

E. Duty Cycle Constraint

DC constraints limit the frequency channel occupancy time of nodes and GW. DC constraints are generally defined in two ways. The first one specifies the period of time when a frequency channel can be occupied during a specific period (e.g., one hour or one day). While this constraint provides high flexibility, such as allowing continuous packet transmission, the definition of a specific period is unclear. Therefore, this paper adopts the second definition, which sets a prohibition period of frequency channel access after packet transmission. When the DC constraint is given by $D_{\mathrm{c}} \in (0,1]$, after transmitting a packet on any frequency channel, the node or GW shall not transmit a packet on the same frequency channel for a period of T^{DC} [sec], calculated as

$$T^{\mathrm{DC}} = \left(\frac{1-D_{\mathrm{c}}}{D_{\mathrm{c}}}\right) T_i^{\mathrm{ToA}}. \tag{5}$$

Since each node does not retransmit a packet, it always satisfies the DC constraint because $G_i^{\mathrm{p}} \gg T_i^{\mathrm{ToA}}$ follows. However, the GW might generate a DL packet during T^{DC}. As shown in Fig. 3, the DL packet is discarded if it cannot be transmitted during the receive window of the node is opening due to the DC constraint.

F. Clock Drift

Generally, the real-time clock (RTC) implemented at a node is not highly accurate, thus causing a deviation from the absolute time. This paper defines the accumulated value of this deviation as clock drift. The clock drift that occurs per unit time is defined as normalized clock drift $\Delta T_i^{\mathrm{cd}}(t)$ at node i, which is randomly determined by a Gaussian distribution $\mathcal{N}(\mu_i, \sigma_i^2)$ with mean μ_i and variance σ_i^2 [30]. Therefore, the clock drift occurring during a specific process T_i^{proc} [sec] at node i is denoted as T_i^{cd} , which is expressed as

$$T_i^{\mathrm{cd}} = \int_0^{T_i^{\mathrm{proc}}} \Delta T_i^{\mathrm{cd}}(t)\,dt. \tag{6}$$

In this study, at nodes, G_i^{p}, $T_{\mathrm{back}}^{\mathrm{cs}}$ and T^{w} are given in (6) as T_i^{proc}, and reflect the effect of clock drift. From now on, variables that reflect the impact of clock drift are denoted with a superscript $(.)^{\star}$.

III. Proposed method

This section explains the resource allocation strategy that overcomes the hidden node problem in LoRaWAN systems. The existing method, RTS/CTS, ensures resources for data packets by transmitting an RTS packet before data packet transmission. However, performance does not improve if the RTS packet collides, and it is essential for the other nodes to listen to the CTS packet more than anything.

Moreover, LPWAN systems face unique constraints compared to other systems, including DC constraints, clock drift, limited receive windows, and topology changes. Our proposed method, an autonomous distributed resource allocation strategy, extends the existing LBT method to overcome the constraints above. In our method, utilizing the periodicity of LPWAN traffic empowers nodes to autonomously perform hidden node recognition, resource allocation, and clock drift compensation triggered by a single DL transmission. Thus, it allows for efficient resource allocation in LPWAN with many nodes subject to DC constraints.

In the proposed method, the GW performs DL transmission control, while the nodes perform clock drift compensation, transmission timing offset allocation, hidden node recognition using CS of DL signals, and frequency channel selection. Hereinafter, we focus on a particular node and omit node index i for simplicity unless otherwise necessary.

The general flow of the proposed method is as follows.

(i) DL transmission control at GW: The GW transmits DL packets if it predicts that the DL transmission can contribute to avoiding packet collisions.

(ii) Clock drift compensation at node: Each node estimates estimated normalized clock drift $\Delta\hat{T}^{\mathrm{cd}}$ based on the reception timestamp of the DL packet during the receive window.

(iii) Resource allocation at node: After executing clock drift compensation, the node performs resource allocation processing aimed at reducing packet collisions caused by the hidden node problem. The main steps involve transmission timing offset T^{off} allocation, implicitly hidden node recognition based on receive window duration CS, which is called RWCS, and frequency channel selection.

A. DL Transmission Criteria

Due to DC constraints, it is challenging to transmit DL packets for all UL packets. Moreover, the GW is unable to receive UL packets while transmitting DL packets. Therefore, the GW transmits DL packets only when it predicts that the corresponding DL transmission can contribute to avoiding packet collisions. When the GW successfully receives a UL packet from a node, the GW can know packet counter FCnt m based on the information included in the packet header. Therefore, the GW can estimate number of lost packets $\hat{N}^{\mathrm{loss}}(j)$ between the $j-1$th and the jth successful receptions from the node. It is crucial to transmit DL packets to nodes that suffer severe packet collisions, implicitly prompting them to reselect resources. Especially in a periodic UL environment, continuous packet collisions of specific node pairs cause the PDR degradation of the entire system [19]. Therefore, it is effective to encourage nodes with persistent packet collisions to change their resource usage. Furthermore, DL packets not only affect the target nodes but also influence the radio resource selection of other nodes performing RWCS (explained in Section III-C3). Considering the above factors, this paper selects the nodes that satisfy the following two conditions as candidates for DL packet transmission.

The first condition is given by

$$\hat{N}^{\mathrm{loss}}(j) \geq 1. \tag{7}$$

The second condition is that *during the jth packet reception processing for node i, no reception processing is being performed on any frequency channel other than frequency channel k_i.*

By the second condition, the nodes that switch frequency channels based on RWCS can reduce the probability of packet collisions on the switched frequency channel. The nodes that satisfy these two conditions become DL transmission candidates. The GW and nodes share T^{w} in advance. Therefore, the GW can estimate the time when the node opens the receive window using T^{w}. If the DC constraint is satisfied at the start of the receive window of the node, the DL packet is transmitted. If the DC constraint is satisfied at the start of the node's receive window, the DL packet is transmitted. If the DC constraint is not met, the DL packet transmission is aborted. Note that the DL packet does not contain any information related to resource allocation.

B. Clock Drift Estimation and Compensation

When a node receives a DL packet in its receive window after transmitting a UL packet, it samples its clock drift. The GW transmits a DL packet after T^{w} [sec] from the reception of the UL packet. However, due to clock drift, the node perceives that it starts receiving the DL packet T^{w} [sec] after the UL packet transmission. Therefore, the node calculates its clock drift $\hat{T}^{\mathrm{d}}_{\ell}$ as

$$\hat{T}^{\mathrm{d}}_{\ell} = \frac{(T_{\mathrm{RS}} - T_{\mathrm{UE}}) - T^{\mathrm{w}}}{T^{\mathrm{w}}}, \quad (8)$$

where ℓ is the index of the number of DL packet reception times, and T_{RS} and T_{UE} are the ℓth DL packet reception start time and UL end time, respectively, given by the clock in the node. Thus,when $\ell > 1$, the estimated normalized clock drift $\Delta\hat{T}^{\mathrm{cd}}$ is obtained as

$$\Delta\hat{T}^{\mathrm{cd}} = \frac{1}{\ell}\sum_{\ell'=1}^{\ell} \Delta\hat{T}^{\mathrm{cd}}_{\ell'}. \quad (9)$$

The node compensates for the clock drift by using $\Delta\hat{T}^{\mathrm{cd}}$ obtained from (9), following the method in [19]. First, the node calculates clock drift compensation value $\hat{T}^{\mathrm{comp}}$ as

$$\hat{T}^{\mathrm{comp}} = \frac{T^{\mathrm{proc}}\Delta\hat{T}^{\mathrm{cd}}}{1 + \Delta\hat{T}^{\mathrm{cd}}}. \quad (10)$$

Then, the node compensates for the impact of clock drift on T^{proc} as

$$T^{\mathrm{proc}} \simeq T^{\mathrm{proc}} - \Delta\hat{T}^{\mathrm{cd}} + \int_{0}^{\left(T^{\mathrm{proc}} - \hat{T}^{\mathrm{cd}}\right)} \Delta T^{\mathrm{cd}}(t)dt. \quad (11)$$

C. Resource Allocation

Figure 4 shows the flowchart of an operation of a node applying the proposed resource allocation strategy. The proposed resource allocation is performed in both time domain and frequency domain. In the time domain, each node decides the transmission timing offset. In the frequency domain, each node selects one of the frequency channels. Figure 5 shows an overview of the frequency channel allocation strategy. The RWCS enables the node to implicitly detect the presence of a hidden node by detecting the DL signal intended for the hidden node.

1) Transmission Timing Offset: Each node determines a transmission timing offset T^{off} to avoid the overlapped transmission timings with the other nodes. When a node receives a DL packet from the GW corresponding to its mth UL packet transmission, the node calculates T^{off} as

$$T^{\mathrm{off}} = t^{\mathrm{back}}_{\mathrm{end}}(m) - t^{\mathrm{g}}(m) - T^{\mathrm{CS}}, \quad (12)$$

where $t^{\mathrm{back}}_{\mathrm{end}}$ [sec] is the CS processing end time, including the backoff processing time for the mth packet, and $t^{\mathrm{g}}(m)$ [sec]

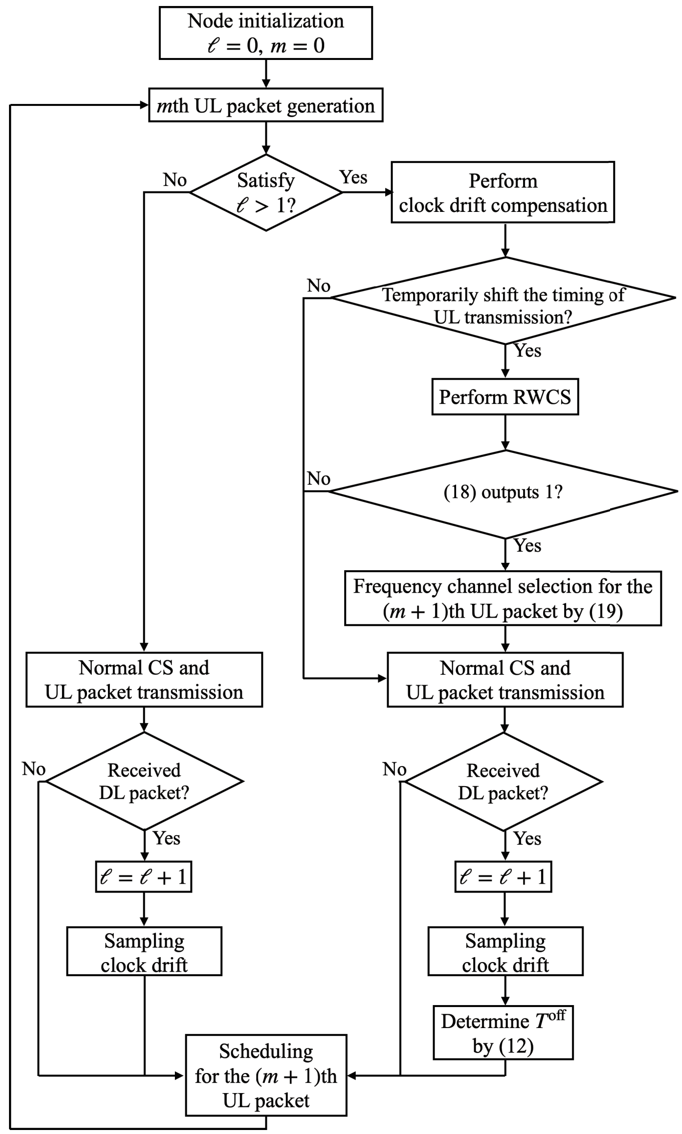

Fig. 4. Flowchart of the node operation.

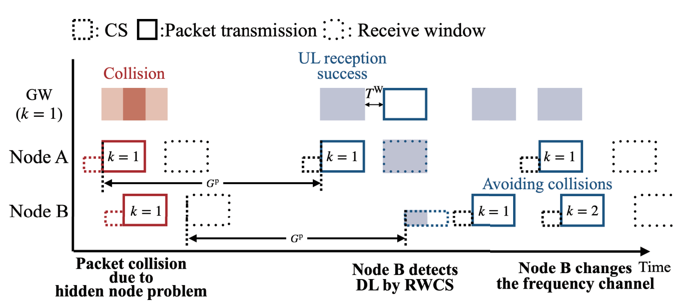

Fig. 5. Overview of the frequency channel allocation strategy.

is the time when the mth UL packet is generated. Therefore, the CS start time $t^{\mathrm{CS}}(m+1)$ [sec] for the $(m+1)$th packet is expressed as

$$t^{\mathrm{CS}}(m+1) = t^{\mathrm{g}}(m+1) + T^{\mathrm{off}}. \quad (13)$$

2) Temporal Timing Shift Probability: All nodes are preassigned a temporary timing shift probability p^{t}. Each node temporarily shifts its packet transmission timing with a probability of p^{t}. The CS start timing $t^{\mathrm{CS}}_{\mathrm{start}}(m)$ for the m-th packet is changed to $t^{\mathrm{CS}}_{\mathrm{start}}(m)+T^{\mathrm{CS}}+T^{\mathrm{ToA}}+2T^{\mathrm{w}}$, at which the performs the CSMA-x operation. Each node changes p^{t} based on the number of DL packets received from the GW as

$$p^{\mathrm{t}} = \begin{cases} P^{\mathrm{t}} & \text{if } l \bmod 2 = 0 \\ 0 & \text{otherwise} \end{cases}, \tag{14}$$

where P^{t} is the initial transmission timing change probability and the function $a \bmod b$ represents the modulo operation, which returns the remainder of a divided by b.

3) Receive Window Duration CS: Each node executes CS during the receive window, i.e., RWCS, in addition to the normal CS of CSMA-x if it decides to shift the transmission timing temporarily. The start time of receive window duration CS, $t^{\mathrm{CS}}_{\mathrm{RW}}(m')$, is expressed as

$$t^{\mathrm{CS}}_{\mathrm{RW}}(m) = t^{\mathrm{CS}}_{\mathrm{start}}(m)+T^{\mathrm{CS}}+T^{\mathrm{ToA}}+T^{\mathrm{w}}. \tag{15}$$

The purpose of the RWCS is to detect the DL packet intended for a hidden node whose UL packet transmission timing overlaps with the UL packet transmission timing. Therefore, the RWCS duration is set to T^{ToA}, which is longer than T^{CS}. By (15), the node can perform CS at the DL packet transmission timing for other nodes that are transmitting UL packets overlapping with its UL packet transmission timing.

In CS, the presence or absence of a signal is detected based on the peak power level in a frequency channel [54]. Therefore, the RWCS only cannot determine if the detected signal is a DL signal from the GW. To address this issue, the node performs energy detection-based CS in RWCS and compares it with the received power of its DL packet, denoted as P^{RDL} [dBm], to detect a DL signal. Suppose an arbitrary complex signal is detected by RWCS. The average signal power, P_v [dBm], observed by RWCS is expressed as

$$P_v = 10\log_{10}\left(\frac{1}{X}\sum_{x=0}^{X-1}\left|v\left[x\right]+n\left[x\right]\right|^2\right), \tag{16}$$

where X is the number of symbols sampled by the node during the RWCS period, $x\left[l\right]$ is the received complex signal, $n\left[l\right]$ is the additive white Gaussian noise (AWGN) following $\mathcal{CN}\left(0,\sigma_n^2\right)$, which is the circularity symmetric complex Gaussian distribution. By comparing the received power of the DL packet intended for the node, P^{RDL} [dBm], with P_v, the node judges the presence of a DL signal. This paper introduces an arbitrary indicator function $f(P_v, P^{\mathrm{RDL}})$. If $f(P_v, P^{\mathrm{RDL}}) = 1$, node i judges that the signal detected by the RWCS is a DL signal.

4) Frequency Channel Selection: Here let $\mathcal{K}' \subseteq \mathcal{K}$ be the set of already selected frequency channels by the node, and let k^* be the newly selected frequency channel. If the node detects the DL signal through (19), it changes the frequency channel for the next packet transmission. The node randomly selects $k^* \in \mathcal{K}\setminus\mathcal{K}'$ and update $\mathcal{K}' = \mathcal{K}' \cup k^*$.

Due to the second condition of DL transmission criteria at the GW, the probability of having nodes transmitting at the overlapping transmit timing can be reduced. If $\mathcal{K}\setminus\mathcal{K}' = \emptyset$, then $\mathcal{K}'$ is initialized to $\emptyset$.

TABLE I
SIMULATION PARAMETERS

Simulation area radius, R	300 [m]
Simulation time	240 [h]
Transmit power, P_{t}	13 [dBm]
Carrier frequency, f_{c}	923 [MHz]
Bandwidth, W	125 [kHz]
Number of frequency channels, K	$\{2, 4, 8\}$
SF, $\mathcal{S}$	7
SNR threshold, Γ^{SNR}	-7.5 [dB]
SIR threshold, Γ^{SIR}	6 [dB]
Coding rate, R	4/7
Duty cycle, D_{c}	0.01
Noise power spectrum density, N_0	-174 [dBm/Hz]
α, β, η	$4.0, 9.5, 4.5$
Overhead symbol, O_{sym}	20.25
Packet data size, B_{data}	160 [bits]
$G^{\mathrm{p}}_{\mathrm{max}}$	5 [min]
$\{\mu_{\mathrm{min}}, \mu_{\mathrm{max}}\}$	$\{-1.91\times10^{-3}$, $0.28\times10^{-3}\}$
$\{\sigma^2_{\mathrm{min}}, \sigma^2_{\mathrm{max}}\}$	$\{9.59\times10^{-11}$, $3.19\times10^{-10}\}$
CS threshold, Γ^{CS}	-110 [dBm]
CS duration, T^{cs}	5 [msec]
$n^{\mathrm{CS}}_{\mathrm{min}}, n^{\mathrm{CS}}_{\mathrm{max}}$	1, 3
T^{w}	5 [sec]
Transmission timing change probability P^{t}	0.05

IV. SIMULATION AND RESULTS

This section provides the comprehensive simulation results of the proposed method against the existing methods.

The nodes are distributed randomly and uniformly within a radius of R [m] centered on the GW. This paper adopts a simple channel model to evaluate the impact on communication quality through resource allocation. The received power, P^{r}_i [dBm], at the GW from node i is expressed as

$$P^{\mathrm{r}}_i = P^{\mathrm{t}} - P^{\mathrm{Loss}}(d_i), \tag{17}$$

where P^{t} [dBm] is the common transmit power for nodes and GW, $P^{\mathrm{Loss}}(d_i)$ [dB] is the path loss with d_i [km] being the physical distance between node i and the GW. The path loss component assumes a non-line-of-sight (NLoS) condition in an urban environment, which is expressed as [55]

$$P_{\mathrm{Loss}}(d_i) = 10\alpha\log_{10} d_i + \beta + 10\eta\log_{10} f_{\mathrm{c}}, \tag{18}$$

where the propagation parameters α, β, and η are the path loss coefficient, offset, and frequency loss component, respectively, and f_{c} [MHz] is the carrier frequency. Assuming a reciprocal channel between the UL and DL channels, the received signal power at node i from the GW is assumed to be equal to P^{r}_i. Furthermore, (17) and (18) are also adopted for the channel model between nodes.

For indicator function $f(P_v, P^{\mathrm{RDL}})$, the following simple function is adopted in this paper for evaluation.

$$f(P_v, P^{\mathrm{RDL}}) = \begin{cases} 1 & \text{if } \mathrm{round}(P_v) = \mathrm{round}(P^{\mathrm{RDL}}) \\ 0 & \text{otherwise} \end{cases}, \tag{19}$$

where $\mathrm{round}(a)$ is a function that rounds a to the nearest integer value.

A. Simulation Parameters

In the simulation, $R = 300$ [m] is set so that the DL signal can be detected by the CS anywhere in the communication area. μ_i and σ_i^2, which determine the normalized clock drift ΔT_i^{d} of node i, are randomly determined from the range $[\mu_{\min}, \mu_{\max}]$, $[\sigma_{\min}^2, \sigma_{\max}^2]$, which were experimentally obtained [30]. The system parameters are listed in Table I, which follow the Japanese parameter configuration AS923 [46].

B. Performance Metrics

1) Packet Delivery Rate: The PDR must be evaluated for a particular observation period owing to periodic traffic. Also, the proposed method performs sequentially, it is necessary to evaluate the time variation of the communication quality of the system. Thus, this paper evaluates the PDR at fixed cycles with a *cycle* being 10 [min]. The PDR during the cth observation period ($c \in \{1, \cdots, c, \cdots, C\}$) is calculated as follows

$$\mathrm{PDR}_c \triangleq \frac{\sum_{i=1}^{I} N_{i,c}^{\mathrm{succ}}}{\sum_{i=1}^{I} N_{i,c}^{\mathrm{tran}}}, \tag{20}$$

where $N_{i,c}^{\mathrm{succ}}$ is the number of UL packets of node i successfully received by the GW during the cth observation period and $N_{i,c}^{\mathrm{tran}}$ is the total number of packets transmitted by node i during the cth observation period.

Furthermore, we evaluate the PDR of each node, expressed as

$$\mathrm{PDR}_i \triangleq \frac{\sum_{c=1}^{C} N_{i,c}^{\mathrm{succ}}}{\sum_{c=1}^{C} N_{i,c}^{\mathrm{tran}}}. \tag{21}$$

2) Packet Reception Cycle: The normalized packet reception cycle (PRC) is adopted to evaluate the impact of continuous packet collisions. The normalized PRC of node i is defined as

$$\mathrm{PRC}_i \triangleq \frac{1}{Z_i - 1} \sum_j \left(\frac{T_{i,j}^{\mathrm{R}} - T_{i,j-1}^{\mathrm{R}}}{G_i^{\mathrm{p}}} \right), \tag{22}$$

where Z_i is the number of UL packets of node i successfully received at the GW and $T_{i,z}^{\mathrm{R}}$ [sec] is the reception time of the jth packet at the GW. Thus, PRC_i became 1 when the GW periodically receives the packets without loss.

C. Numerical Results

1) PDR Performance: Figure 6 shows the performance of PDR_c for $I = 1000$ nodes. From this figure, the proposed method can improve the PDR performance over time regardless of the number of frequency channels K. This is because the proposed method enables an increasing number of nodes to use radio resources that can avoid packet collisions caused by the hidden node problem. The proposed method effectively performs resource allocation in the time domain using transmission timing offset, even in asynchronous systems, by conducting sequential clock drift compensation. Furthermore, selecting frequency channels based on RWCS can avoid any packet collisions that cannot be avoided in the time domain. As a result, with the number of frequency channels $K = 2$, the proposed method can improve the PDR performance by up to approximately 9% and 8% compared to CSMA-x and LMAC, respectively. Here, LMAC provides no significant improvement over CSMA-x. This is because both CSMA-x and LMAC are unable to avoid packet collisions that occur due to the hidden node problem. When wireless resources are sufficient for the given system traffic load, the majority of packet loss in LBT-based methods is caused by the hidden nodes. Thus, tackling the hidden node problem is essential to improve the PDR performance. On the other hand, when $K = 4$ or 8, the proposed method experiences a temporary decrease in PDR immediately after the system starts. This is due to the influence of the DL transmission criteria and clock drift. When $K = 4, 8$, there are sufficient resources relative to the traffic load, resulting in a low packet collision rate. As a result, fewer nodes are subject to DL transmissions, and fewer nodes have active clock drift compensation. Thus, the relative transmission timing drift over time between nodes with and without clock drift compensation becomes smaller, making it more likely for continuous packet collisions to occur.

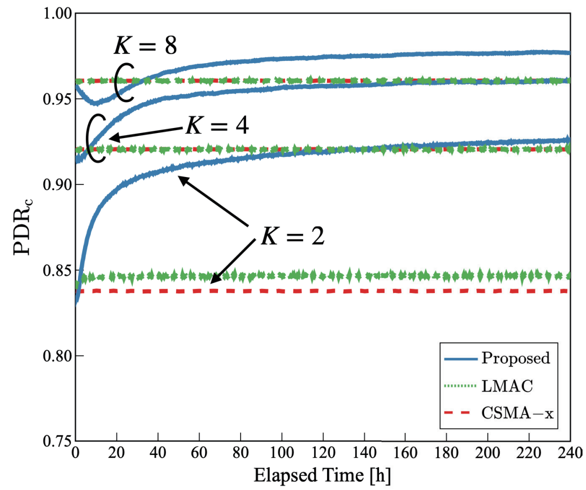

Fig. 6. PDR_c for $I = 1000$

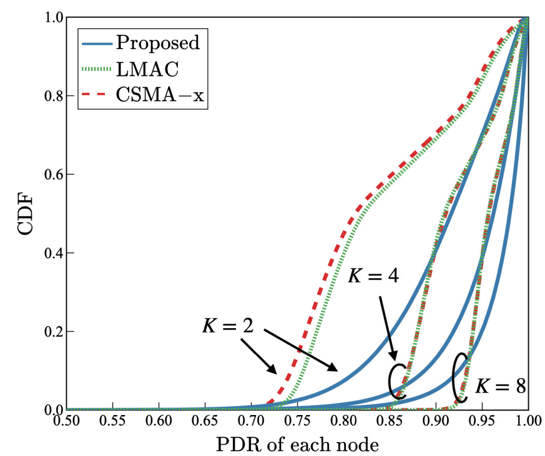

Fig. 7. CDF of the PDR per node for $I = 1000$

Figure 7 shows the cumulative distribution function (CDF)

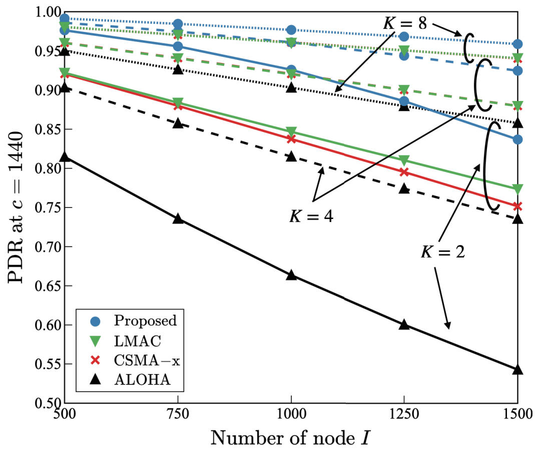

Fig. 8. Impact of the PDR per number of nodes at $c = 1440$

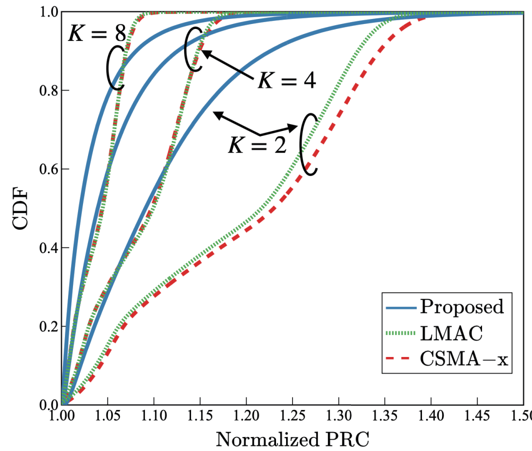

Fig. 9. CDF of the PRC for $I = 1000$

of the PDR performance for each node. From Fig. 7, the proposed method can shift the curve to the right and increase the ratio of nodes achieving high PDR. However, when $K = 4$ or 8, the tail of the CDF of the proposed method is flaring out compared to that of CSMA-x and LMAC. This is because of the influence of nodes affected by the aforementioned continuous packet collisions.

Figure 8 shows the PDR_c as a function of the number of nodes at period $c = 1440$. As shown in Fig. 8, the proposed method improves the PDR performance compared to pure ALOHA, CSMA-x and LMAC, regardless of the number of frequency channels or nodes. In particular, the proposed method can improve the PDR performance by up to approximately 29%, 9% and 8% compared to pure ALOHA when $I = 1500$ and $K = 2$, CSMA-x when $I = 1000, 1250$ and $K = 2$, and LMAC when $I = 1000$ and $k = 2$, respectively. Moreover, the proposed method achieves a higher PDR when $I = 1000, K = 2$ than LMAC with $I = 500, K = 2$, indicating that the capacity of the number of nodes has more than doubled. Since high PDR is required for the system, the proposed method increases the number of capacity nodes compared to LMAC for all numbers of frequency channels.

2) PRC Performance: From Fig. 9, the proposed method could increase the ratio of nodes with low PRC compared to CSMA-x and LMAC, despite the transmission delay caused by the transmission timing offset and temporary changes in transmission timing. This is because the packet generation cycle is much larger than the transmission delay caused by the proposed method, making the effect of avoiding continuous packet collisions more pronounced.

3) Additional Evaluation: Here, as an additional evaluation, we show the performance when the topology changes and when clock drift compensation is ideally performed.

In LPWAN, the network topology may change unintentionally due to factors such as battery depletion of nodes. Therefore, we evaluate the robustness of the proposed method against topology changes. We evaluate a scenario where 10% or 20% of the nodes randomly selected stop working and then restart after some time. These nodes transition to a stop state at random times between 80 and 92 hours after the system starts and restart operation at random times between 104 and 116 hours. Note that the stopped nodes initialize their communication parameters, including the clock drift estimation values. Figure 10 shows the PDR performance of the proposed method when the topology changes. From Fig. 10, even when the topology changes, the proposed method could asymptotically converge to the same PDR performance as in the case without topology changes over time. This is because each node performs sequential resource selection triggered by DL packets. In particular, since the DL transmission criteria of the proposed method are affected by the packet collision rate, the proposed method can indirectly reflect the impact of topology changes for the resource selection of nodes. Therefore, the proposed method is robust against topology changes.

Finally, we evaluate the PDR performance in the case where ideal clock drift compensation is possible. This case corresponds to situations where clock drift is compensated by including control information in the DL packets or when the number of clock drift samples ℓ obtained by the proposed method becomes sufficiently large. Figure 11 shows the PDR performance of the proposed method with the ideal clock drift compensation. Here, ''Proposed with ideal comp.'' represents the performance when $\Delta\hat{T}^{\mathrm{cd}} = \Delta T^{\mathrm{cd}}$ holds for nodes satisfying $\ell > 1$. From Fig. 11, when the accuracy of clock drift compensation improves, the proposed method could further enhance the PDR performance. In particular, ''Proposed with ideal comp.'' achieves a PDR of over 95% when $K = 2$. Therefore, if the system allows the overhead of including control information such as timestamps in the DL packets, The proposed method could improve the PDR performance by up to approximately 13% and 12% compared to CSMA-x and LMAC when $I = 1000$ and $K = 2$, respectively.

V. Conclusion

This paper focused on the hidden node problem in LPWAN with CS and proposed an autonomous distributed resource allocation strategy to mitigate packet collision by the hidden node problem. In the proposed method, each node performs sequential clock drift estimation and compensation,

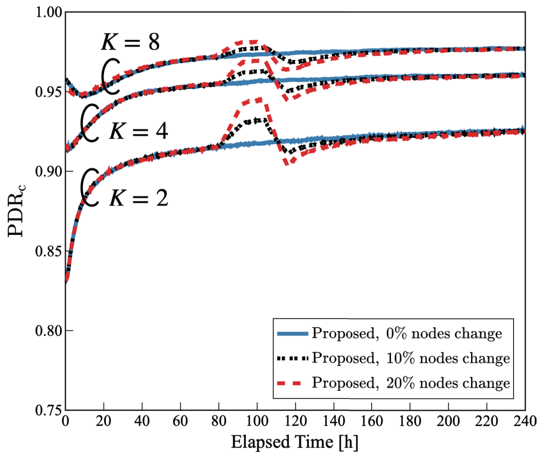

Fig. 10. PDR$_c$ for I = 1000 with topology change

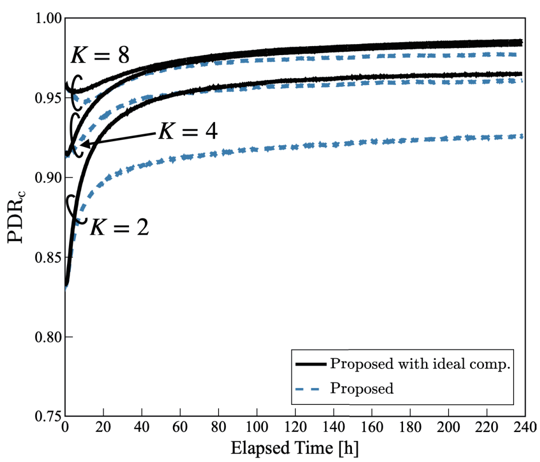

Fig. 11. PDR$_c$ for I = 1000 with ideal compensation of clock drift

and detects the existence of hidden nodes through receive window duration carrier sense (RWCS). By leveraging the periodic traffic and RWCS, the nodes implicitly recognize the presence of hidden nodes and reselect frequency channels, thereby reducing packet collisions caused by the hidden node problem. Extensive numerical evaluation has elucidated that the proposed method can improve the PDR performance by up to approximately by 29%, 9% and 8% compared to ALOHA, CSMA-x, and LoRa MAC, respectively. Thus, the proposed approach can mitigate the hidden node problem under the unique constraints of LPWAN, such as DC and limited receive window.

However, the design of the proposed method is based on a static channel environment in which nodes and GW are assumed to be in fixed locations. In addition, other systems may exist in the unlicensed band used by LPWAN. Therefore, it is important for future LPWANs to provide simple signal detection technology at nodes that can accurately detect DL signals even in a dynamic channel environment or in the presence of other systems.

References

[1] O. Khutsoane, B. Isong, and A. M. Abu-Mahfouz, ''IoT Devices and Applications Based on LoRa/LoRaWAN,'' *in Proc. 43rd Annu. Conf. IEEE Ind. Electron. Soc. (IECON)*, pp. 6107–6112, 2017.

[2] M. Ballerini, T. Polonelli, D. Brunelli, M. Magno, and L. Benini, ''NB-IoT Versus LoRaWAN: An Experimental Evaluation for Industrial Applications,'' *IEEE Trans. Industr. Inform.*, vol. 16, no. 12, pp. 7802–7811, 2020.

[3] K. Mekki, E. Bajic, F. Chaxel, and F. Meyer, ''Overview of Cellular LPWAN Technologies for IoT Deployment: Sigfox, LoRaWAN, and NB-IoT,'' *in Proc. IEEE Int. Conf. Pervasive Comput. Commun. Workshops (PerCom Workshops)*, pp. 197–202, 2018.

[4] M. T. Abbas, K.-J. Grinnemo, J. Eklund, S. Alfredsson, M. Rajiullah, A. Brunstrom, G. Caso, K. Kousias, and O. Alay, ''Energy-Saving Solutions for Cellular Internet of Things–A Survey,'' *IEEE Access*, vol. 10, pp. 62 073–62 096, 2022.

[5] M. Jouhari, N. Saeed, M.-S. Alouini, and E. M. Amhoud, ''A Survey on Scalable LoRaWAN for Massive IoT: Recent Advances, Potentials, and Challenges,'' *IEEE Commun. Surveys & Tut.*, vol. 25, no. 3, pp. 1841–1876, 2023.

[6] O. Georgiou and U. Raza, ''Low Power Wide Area Network Analysis: Can LoRa Scale?'' *IEEE Commun. Lett.*, vol. 6, no. 2, pp. 162–165, 2017.

[7] W. Guibene, J. Nowack, N. Chalikias, K. Fitzgibbon, M. Kelly, and D. Prendergast, ''Evaluation of LPWAN Technologies for Smart Cities: River Monitoring Use-Case,'' *2017 IEEE Wireless Commu. Netw. Conf. Workshops (WCNCW)*, pp. 1–5, 2017.

[8] U. Raza, P. Kulkarni, and M. Sooriyabandara, ''Low Power Wide Area Networks: An Overview,'' *IEEE Commun. Surveys & Tut.*, vol. 19, no. 2, pp. 855–873, 2017.

[9] R. Marini, K. Mikhaylov, G. Pasolini, and C. Buratti, ''Low-Power Wide-Area Networks: Comparison of LoRaWAN and NB-IoT Performance,'' *IEEE Internet Things J.*, vol. 9, no. 21, pp. 21 051–21 063, 2022.

[10] R. K. Verma, S. Bharti, and K. K. Pattanaik, ''GDA: Gravitational Data Aggregation Mechanism for Periodic Wireless Sensor Networks,'' *in Proc. 2018 IEEE SENSORS*, pp. 1–4, 2018.

[11] V. Gupta, S. K. Devar, N. H. Kumar, and K. P. Bagadi, ''Modelling of IoT Traffic and Its Impact on LoRaWAN,'' *in Proc. IEEE GLOBECOM*, pp. 1–6, Dec. 2017.

[12] Z. Xu, J. Luo, Z. Yin, T. He, and F. Dong, ''S-MAC: Achieving High Scalability via Adaptive Scheduling in LPWAN,'' *in Proc. IEEE INFOCOM 2020*, pp. 506–515, 2020.

[13] A. H. Nguyen, Y. Tanigawa, and H. Tode, ''Scheduling Method for Solving Successive Contentions of Heterogeneous Periodic Flows Based on Mathematical Formulation in Multi-Hop WSNs,'' *IEEE Sens. J.*, vol. 18, no. 21, pp. 9021–9033, 2018.

[14] A. Kaburaki, K. Adachi, O. Takyu, M. Ohta, and T. Fujii, ''Resource Allocation for Periodic Traffic in Wireless Sensor Network,'' *in Proc. IEEE WCNC International Workshop on Smart Spectrum (IWSS 2023)*, 2023.

[15] Z. Qin and J. A. McCann, ''Resource Efficiency in Low-Power Wide-Area Networks for IoT Applications,'' *in Proc. IEEE GLOBECOM*, pp. 1–7, Dec. 2017.

[16] J. Ortín, M. Cesana, and A. Redondi, ''Augmenting LoRaWAN Performance With Listen Before Talk,'' *IEEE Trans. Wireless Commun.* , vol. 18, no. 6, pp. 3113–3128, Jun. 2019.

[17] A. Kaburaki, K. Adachi, O. Takyu, M. Ohta, and T. Fujii, ''Autonomous Decentralized Traffic Control Using Q-Learning in LPWAN,'' *IEEE Access*, vol. 9, pp. 93 651–93 661, 2021.

[18] J. Haxhibeqiri, I. Moerman, and J. Hoebeke, ''Low Overhead Scheduling of LoRa Transmissions for Improved Scalability,'' *IEEE Internet Things J.*, vol. 6, no. 2, pp. 3097–3109, 2019.

[19] A. Kaburaki, K. Adachi, O. Takyu, M. Ohta, and T. Fujii, ''Adaptive Resource Allocation Utilizing Periodic Traffic and Clock Drift in LPWAN,'' *IEEE Trans. Wireless Commun.* , vol. 23, no. 4, pp. 3795–3807, 2024.

[20] L. Beltramelli, A. Mahmood, P. Österberg, and M. Gidlund, ''LoRa Beyond ALOHA: An Investigation of Alternative Random Access Protocols,'' *IEEE Trans. Ind. Informat.*, vol. 17, no. 5, pp. 3544–3554, 2021.

[21] C. Pham, ''Investigating and experimenting CSMA channel access mechanisms for LoRa IoT networks,'' *in Proc. IEEE Wireless Commun. Netw. Conf. (WCNC)*, pp. 1–6, 2018.

[22] N. Kouvelas, V. Rao, and R. Prasad, ''Employing p-CSMA on a LoRa Network Simulator,'' *arXiv preprint arXiv:1805.12263*, 2018.

[23] Q. L. Hoang and H. Oh, ‘‘A Real-Time LoRa Protocol Using Logical Frame Partitioning for Periodic and Aperiodic Data Transmission,’’ *IEEE Internet Things J.*, vol. 9, no. 16, pp. 15 401–15 412, 2022.
[24] J. Pullmann and D. Macko, ‘‘A New Planning-Based Collision-Prevention Mechanism in Long-Range IoT Networks,’’ *IEEE Internet Things J.*, vol. 6, no. 6, pp. 9439–9446, 2019.
[25] M. Moltafet, M. Leinonen, and M. Codreanu, ‘‘Worst Case Age of Information in Wireless Sensor Networks: A Multi-Access Channel,’’ *IEEE Wireless Commun. Lett.*, vol. 9, no. 3, pp. 321–325, 2020.
[26] S. Kaul, M. Gruteser, V. Rai, and J. Kenney, ‘‘Minimizing Age of Information in Vehicular Networks,’’ *in Proc.2011 8th Annu. IEEE Commun. Soc. Conf. on Sensor, Mesh and Ad Hoc Commun. and Netw.*, pp. 350–358, 2011.
[27] S. Kaul, R. Yates, and M. Gruteser, ‘‘Real-Time Status: How Often Should One Update?’’ *in Proc. 2012 IEEE INFOCOM*, pp. 2731–2735, 2012.
[28] R. D. Yates and S. K. Kaul, ‘‘The Age of Information: Real-Time Status Updating by Multiple Sources,’’ *IEEE Trans. Inf. Theory*, vol. 65, no. 3, pp. 1807–1827, 2019.
[29] D. Djenouri and M. Bagaa, ‘‘Synchronization Protocols and Implementation Issues in Wireless Sensor Networks: A Review,’’ *IEEE Syst. J.*, vol. 10, no. 2, pp. 617–627, 2016.
[30] K. Tsurumi, A. Kaburaki, K. Adachi, O. Takyu, M. Ohta, and T. Fujii, ‘‘Simple Clock Drift Estimation & Compensation for Packet-Level Index Modulation and its Implementation in LoRaWAN,’’ *IEEE Internet Things J.*, 2022.
[31] L. Tessaro, C. Raffaldi, M. Rossi, and D. Brunelli, ‘‘Lightweight Synchronization Algorithm with Self-Calibration for Industrial LORA Sensor Networks,’’ in *2018 Workshop on Metrology for Industry 4.0 and IoT*, 2018, pp. 259–263.
[32] C. Garrido-Hidalgo, J. Haxhibeqiri, B. Moons, J. Hoebeke, T. Olivares, F. J. Ramirez, and A. Fernández-Caballero, ‘‘LoRaWAN Scheduling: From Concept to Implementation,’’ *IEEE Internet Things J.*, vol. 8, no. 16, pp. 12 919–12 933, 2021.
[33] T. Polonelli, D. Brunelli, A. Marzocchi, and L. Benini, ‘‘Slotted ALOHA on LoRaWAN-Design, Analysis, and Deployment,’’ *Sensors*, vol. 19, no. 4, p. 838, 2019.
[34] T. Polonelli, D. Brunelli, and L. Benini, ‘‘Slotted ALOHA Overlay on LoRaWAN - A Distributed Synchronization Approach,’’ *in Proc. IEEE 16th Int. Conf. Embedded Ubiquitous Comput. (EUC)*, pp. 129–132, 2018.
[35] Loh, Frank and Raunecker, David and Hoβfeld, Tobias, ‘‘Assessment of Optimal Time Scheduled Channel Access in LoRaWAN,’’ *in Proc. IEEE Int. Conf. Commun. (ICC)*, pp. 300–305, 2024.
[36] T.-H. To and A. Duda, ‘‘Simulation of LoRa in NS-3: Improving LoRa Performance with CSMA,’’ *in Proc. IEEE Int. Conf. Commun. (ICC)*, pp. 1–7, 2018.
[37] Gamage, Amalinda and Liando, Jansen and Gu, Chaojie and Tan, Rui and Li, Mo, ‘‘LMAC: Efficient Carrier-Sense Multiple Access for LoRa,’’ *in Proc. 26th Annu. Int. Conf. Mobile Comput. Netw.*, no. 43, pp. 1–27, 2020.
[38] Gamage, Amalinda and Liando, Jansen and Gu, Chaojie and Tan, Rui and Li, Mo and Seller, Olivier, ‘‘LMAC: Efficient Carrier-Sense Multiple Access for LoRa,’’ *ACM Transactions on Sensor Networks*, vol. 19, no. 2, pp. 1–27, 2023.
[39] R. Fernandes, M. Luís, and S. Sargento, ‘‘Large-Scale LoRa Networks: A Mode Adaptive Protocol,’’ *IEEE Internet Things J.*, vol. 8, no. 17, pp. 13 487–13 502, 2021.
[40] R. Fernandes, R. Oliveira, M. Luís, and S. Sargento, ‘‘Exploring the Use of Control Packets in LoRa Medium Access: A Scalability Analysis,’’ *in Proc. IEEE 21st Int. Symp. World Wireless Mobile Multimedia Netw. (WoWMoM)*, pp. 1–7, 2020.
[41] C. Pham and M. Ehsan, ‘‘Dense Deployment of LoRa Networks: Expectations and Limits of Channel Activity Detection and Capture Effect for Radio Channel Access,’’ *Sensors*, vol. 21, no. 3, p. 825, 2021.
[42] LoRa Alliance, ‘‘TR013-1.0.0 Carrier Sense Multiple Access (CSMA),’’ [online]Available:https://resources.lora-alliance.org/technical-recommendations/tr013-1-0-0-csma.
[43] R. Oliveira, L. Guardalben, M. Luis, and S. Sargento, ‘‘Multi-Technology Data Collection: Short and Long Range Communications,’’ in *2017 IEEE 86th Vehicular Technology Conference (VTC-Fall)*, 2017, pp. 1–6.
[44] A. Kaburaki, K. Adachi, O. Takyu, M. Ohta, and T. Fujii, ‘‘LBT-based Resource Allocation Methods Utilizing Periodicity of Traffic in LPWAN,’’ in *Proc. Int. Conf. on Computing, Netw. and Commun. (ICNC 2024)*, 2024.
[45] B. Reynders, W. Meert, and S. Pollin, ‘‘Range and coexistence analysis of long range unlicensed communication,’’ *in Proc. 2016 23rd Int. Conf. on Telecommun. (ICT)*, pp. 1–6, 2016.
[46] LoRa Alliance, ‘‘RP002-1.0.4 Regional Parameters,’’ [online]Available:https://resources.lora-alliance.org/technical-specifications/rp002-1-0-4-regional-parameters.
[47] D. Bankov, E. Khorov, and A. Lyakhov, ‘‘On the Limits of LoRaWAN Channel Access,’’ *in 2016 Int. Conf. on Engineering and Telecommun. (EnT)*, pp. 10–14, 2016.
[48] L. Vangelista, ‘‘Frequency Shift Chirp Modulation: The LoRa Modulation,’’ *IEEE Signal Process. Lett.*, vol. 24, no. 12, pp. 1818–1821, 2017.
[49] C. Shao and O. Muta, ‘‘When LoRaWAN Meets CSMA: Trends, Challenges, and Opportunities,’’ *IEEE Internet Things Mag.*, vol. 7, no. 1, pp. 90–96, 2024.
[50] Semtech, ‘‘Semtech SX1272 Datasheets,’’ [online]. Available:https://www.semtech.com/products/wireless-rf/lora-core/sx1272.
[51] LoRa Alliance, ‘‘TS001-1.0.4 LoRaWAN® L2 1.0.4 Specification,’’ [online]Available:https://resources.lora-alliance.org/technical-specifications/ts001-1-0-4-lorawan-l2-1-0-4-specification.
[52] D. Croce, M. Gucciardo, S. Mangione, G. Santaromita, and I. Tinnirello, ‘‘Impact of LoRa Imperfect Orthogonality: Analysis of Link-Level Performance,’’ *IEEE Commun. Lett.*, vol. 22, no. 4, pp. 796–799, Apr. 2018.
[53] A. Waret, M. Kaneko, A. Guitton, and N. El Rachkidy, ‘‘LoRa Throughput Analysis With Imperfect Spreading Factor Orthogonality,’’ *IEEE Wireless Commun. Lett.*, vol. 8, no. 2, pp. 408–411, 2019.
[54] S. Narieda and T. Fujii, ‘‘Energy Detection Based Carrier Sense in LPWAN,’’ *IEEE Access*, vol. 11, pp. 79 105–79 119, 2023.
[55] P. Series, ‘‘Propagation Data and Prediction Methods for the Planning of Short-Range Outdoor Radiocommunication Systems and Radio Local Area Networks in the Frequency Range 300 MHz to 100 GHz,’’ [online]. Available:https://www.itu.int/rec/R-REC-P.1411-9-201706-S/en, 2017.

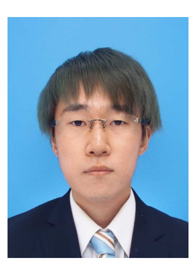

Aoto Kaburaki received the B.E. and M.E. degree in information and communication engineering from The University of Electro-Communications, Japan, in 2020 and 2022 respectively, where he is currently pursuing the Ph.D. degree. His research interests include machine learning and its application to wireless communication.

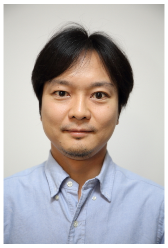

Koichi Adachi received the B.E., M.E., and Ph.D. degrees in engineering from Keio University, Japan, in 2005, 2007, and 2009 respectively. His research interests include cooperative communications and energy efficient communication technologies.

From 2007 to 2010, he was a Japan Society for the Promotion of Science (JSPS) research fellow. He was the visiting researcher at City University of Hong Kong in April 2009 and the visiting research fellow at University of Kent from June to Aug 2009. From May 2010 to May 2016, he was with the Institute for Infocomm Research, A*STAR, in Singapore. Currently, he is an associate professor at The University of Electro-Communications, Japan. He served as General Co-chair of the 10th and 11th IEEE Vehicular Technology Society Asia Pacific Wireless Communications Symposium (APWCS), Track Co-chair of Transmission Technologies and Communication Theory of the 78th and 80th IEEE Vehicular Technology Conference in 2013 and 2014, respectively, and symposium co-chair of communication theory symposium of IEEE Globecom 2018, Tutorial Co-Chair of IEEE ICC 2019, and symposium co-chair of wireless communications symposium of IEEE Globecom 2020. He was an Associate Editor of IET Transactions on Communications between 2015 – 2017, IEEE Wireless Communications Letters since 2016, IEEE Transactions on Vehicular Technology between 2016 – 2018, IEEE IEEE Transactions on Green Communications and Networking since 2016, and IEEE Open Journal of Vehicular Technology since 2019. He is a member of the IEICE.

He was recognized as the Exemplary Reviewer from IEEE Wireless Communications Letters in 2012, 2013, 2014, and 2015. He was awarded excellent editor award from IEEE ComSoc MMTC in 2013. He is a co-author of WPMC2020 Best Student Paper Award.

Osamu Takyu received the B.E. degree in Electrical Engineering from Tokyo University of Science, Chiba, Japan, in 2002 and the M.E. and Ph. D. degrees in Open and Environmental Systems from Keio University, Yokohama, Japan in 2003 and 2006, respectively. From 2003 to 2007, he was a research associate in the Department of Information and Computer Science, Keio University. From 2004 to 2005, he was visiting scholar in the School of Electrical and Information Engineering, University of Sydney. From 2007 to 2011, he was an assistant professor in the Department of Electrical Engineering, Tokyo University of Science. He was an assistant professor from 2011 to 2013, an associate professor from 2013 to 2023, and has been a professor from 2023 in the Department of Electrical & Computer Engineering, Shinshu University. Dr. Osamu TAKYU is a recipient of the Young Researcher's award of IEICE 2010, 2010 Active Research Award in Radio Communication Systems from IEICE technical committee on RCS, and 2018 Best Paper Award in Smart Radio form IEICE technical committee on SR. His current research interests are in wireless communication systems and distributed wireless communication technology. He is a member of IEEE.